Subspace-based 1-bit Wideband Spectrum Sensing

Junquan Deng, Yong Chen
The Sixty-third Research Institute, National University of Defence Technology, Nanjing, China

***Abstract*—We consider spectrum sensing in a wideband cognitive radio system where 1-bit analog-to-digital converters (ADCs) are adopted at the radio frequency (RF) sensors. We focus on a practical scenario where multiple narrow-band radio systems coexist in the considered wide spectrum range and the RF sensor has no prior knowledge about those ambient radio systems. First, we use Van Vleck's arcsine law to analyze the impact of 1-bit sampling on performance of covariance matrix reconstruction. Second, we propose a novel 1-bit wideband spectrum sensing algorithm based on the subspace technique. We show that the proposed method exhibits near-zero false alarm (FA) while achieves the similar probability of detection (PD) performance as compared to conventional FFT-based and correlation-based wideband sensing methods.**

***Index Terms*—spectrum sensing, one-bit ADC, sub-space method, false alarm, probability of detection**

I. Introduction

Spectrum sensing [1] for the radio frequency (RF) environment is a fundamental problem in a cognitive radio (CR) system. However, how to learn the spectrum occupancy state for a wideband system in a fast and energy-efficient way is still a challenging problem [2], especially in a cognitive radio sensor network (CRSN) [3] where low hardware costs and low power consumption are required. The main objective of wideband spectrum sensing is to simultaneously detect the occupation states of individual slices in a wide frequency band which could be several GHz. Wideband spectrum sensors with high time-resolutions are expensive and power-hungry due to the use of high-speed analog-to-digital converters (ADC), and large amounts of computing & caching resources for performing real-time signal processing.

To deploy a wideband spectrum sensor network at a large scale for monitoring the RF spectrum states in a geographic area, one should use low-cost and low-power-consumption RF sensors. ADCs play a central role in digital sensing and communication systems. They account for a considerable hardware cost and energy consumption for an RF sensor or receiver. The circuit complexity and the power consumption of a ADC grows exponentially $\mathcal{O}(2^b)$ with the sampling resolution in the form of the number of bits b. Towards low-cost wideband RF sensing, a promising option is to switch from Nyquist high-resolution data sampling to data acquisition with coarse ADC resolutions. A radical approach is to adopt 1-bit ADCs which acquire only the signs of analog receive signals and discard the amplitude information.

A. Relevant Art

Low-resolution ADCs, especially 1-bit ADCs have been considered for massive MIMO communication systems [4], [5], low-cost radar systems [6], [7], and direction of arrival (DoA) estimation [8], [9]. It is known that performances of signal estimation and detection using 1-bit ADCs incurs only a small loss as compared to high-resolution ADCs in the low-SNR regime. In fact, when SNR is low, high-resolution ADCs are unnecessary as the sampled data contain few information about the signal which is overwhelmed by the noise. The theories behind using 1-bit ADCs for various signal estimation and detection applications date back to the pioneering work by Van Vleck in analyzing the power spectrum of amplitude-clipped Gaussian noise, and the famous Bussgang's theorem for the cross-correlation of a Gaussian signal and its nonlinear distorted version. The problem of narrow-band frequency estimation from 1-bit quantized samples was investigated in [10], where the the effects of 1-bit sampling and quantization on frequency estimation for a single-tone signal are studied. Wideband spectrum sensing with 1-bit ADCs was considered in [11], where the power spectral density (PSD) is estimated based on the 1-bit sampled data via Discrete Fourier transform (DFT).

B. Contributions and Outline

We consider using one-bit ADCs for blind wideband spectrum sensing. Based on the classical arcsine law for 1-bit quantized signals, we propose a low-complexity yet efficient spectrum detection algorithm via a modified Multiple Signal Classification (MUSIC) method. Compared to existing methods, the proposed one shows superior detection performances. In Section II, we present the system framework, signal model, and formulate the problem. In Section III, we use Van Vleck's arcsine law to analyze the effects of 1-bit quantization. In Section IV, we detail the proposed subspace-based 1-bit sensing method. In Section V, we demonstrate the efficacy of the proposed 1-bit wideband sensing method via numerical simulation. Finally, we conclude the paper in Section VI.

II. System Model and Problem Formulation

We consider a spectrum monitoring system where RF sensors with high-speed 1-bit ADCs are adopted to monitor a wide RF band. The interested RF band is $(f_c - F_s/2, f_c + F_s/2)$, with f_c the frequency of the RF oscillator, and F_s the ADC sampling rate. We assume that the ambient RF systems operate over a GHz-wide band which can be divided into N sub-bands (slices). The N sub-bands are assumed to have a same bandwidth B. The values of N and B are deliberately chosen so that $F_s = NB$. Each primary user (PU) in the systems operates on one sub-band and it is assumed that there are M ($M < N$) active PUs at a time.

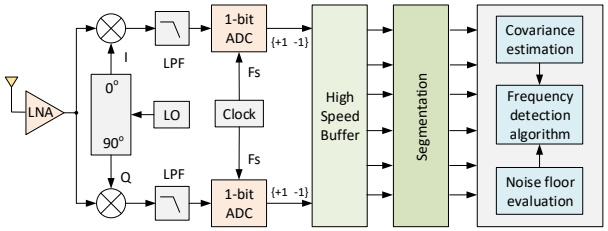

Fig. 1. System architecture for 1-bit wideband spectrum sensing where a homodyne RF receiver with a pair of 1-bit ADCs are adopted.

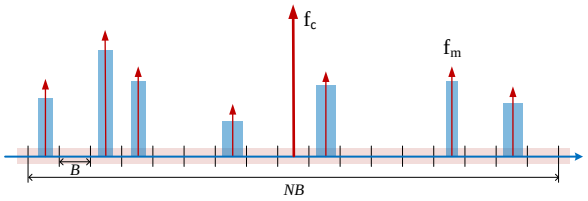

Fig. 2. Slicing for a wideband spectrum range.

A. Hardware Architecture

The considered 1-bit RF sensor hardware architecture is depicted as in Fig. 1, where a homodyne RF receiver with a pair of 1-bit ADCs are adopted to acquire both the highly clipped versions of the in-phase (I) and quadrature (Q) signals. In practice, 1-bit ADCs can be implemented using a single comparator [12], which has an ultra-low driving power. It should be stressed that the homodyne RF architecture has reduced circuit complexity and power consumption, and is naturally suited to 1-bit sampling as no automatic gain control (AGC) is required for the RF amplifier. At the baseband signal processing part, a high-speed buffer is used to store the sampled data, i.e., signs of the realtime I/Q signals. Due to the extreme quantization, the size of the buffer can also be greatly reduced. The bits in the buffer will then be segmented into snapshots and forwarded to the baseband signal processor where spectrum sensing algorithms are implemented. Due to the simplicity in 1-bit data operation, the signal processing complexity would be much lower than that for conventional high-resolution sampled data.

B. Signal Model

The interested spectrum band of width NB is intentionally divided into N slices so that the frequency-domain resolution achieved by a wideband spectrum sensing method is lower than B. In the time domain, this is accomplished by segmenting the 1-bit clipped signal into non-overlapped snapshots with length of exactly N samples. We assume that the operational baud rates for the ambient RF systems is smaller or equal to B. Assuming $F_s \gg B$, the PU signals will be narrow-band and can be approximately treated as a complex sinusoid [13] from the wideband sensing perspective. Due to the ultra high 1-bit sampling rate, the M narrow-band signals can be represented by complex frequency tones with different center frequencies $\{f_m\}_{m=1}^M$. As a result, the continuous-time received signals at the RF sensor before sampling can be written as

$$y(t) = \sum\nolimits_{m=1}^{M} \alpha_m(t) e^{\mathbf{j}2\pi f'_m(t-\tau_m)} + w(t), \tag{1}$$

where $f'_m = f_m - f_c$ is the baseband frequency for the m-th narrow-band signal, $\mathbf{j} = \sqrt{-1}$, $\alpha_m(t)$ represents the complex envelope which depends on the channel coefficient and the PU signalling mechanism, and τ_m represents the random relative delay within the observation window of length $T = N/F_s$, and $w(t) \sim \mathcal{CN}(0, \sigma_w^2)$ is the circularly symmetric complex Gaussian (CSCG) noise with variance σ_w^2 and zero mean. The coefficients $\{\alpha_m(t)\}_{m=1}^M$ for M signals are assumed to be independent identically distributed (i.i.d) as the radio propagation channels between the RF sensor and the M PUs are independent. Throughout the analysis, we assume that the RF sensor has no prior knowledge about the structure of the signals, and the coefficients $\{\alpha_m(t)\}_{m=1}^M$ can be treated as random variables drawn from $\mathcal{CN}(0, \sigma_s^2)$ with zero mean and power σ_s^2. Based on (1), the unquantized discrete signals with sampling rate F_s is

$$y[n] = \sum\nolimits_{m=1}^{M} \alpha_m[n] e^{\mathbf{j}2\pi f'_m\left(\frac{n}{F_s} - \tau_m\right)} + w[n], \tag{2}$$

with $\alpha_m[n] = \alpha_m(n/F_s)$ and $w[n] = w(n/F_s)$, and $n \in \mathbb{Z}$. The 1-bit quantized signal is then given by

$$q[n] = \mathcal{Q}(y[n]), \tag{3}$$

where $\mathcal{Q}(\cdot)$ represent the 1-bit quantization function for a complex signal, and it is given by

$$\mathcal{Q}(z) = \frac{1}{\sqrt{2}} \left(\text{sign}(\Re\{z\}) + \mathbf{j}\,\text{sign}(\Im\{z\})\right), \tag{4}$$

with $\Re\{z\}$ and $\Im\{z\}$ the real part and the imaginary part of a complex number z, respectively. Clearly, the value of $q[n]$ is from a QPSK constellation $\{\frac{1+\mathbf{j}}{\sqrt{2}}, \frac{1-\mathbf{j}}{\sqrt{2}}, \frac{-1+\mathbf{j}}{\sqrt{2}}, \frac{-1-\mathbf{j}}{\sqrt{2}}\}$. Stacking N samples in one snapshot, we have an unquantized received vector

$$\mathbf{y} = \mathbf{s} + \mathbf{w} = [y[0], y[1], \cdots, y[N-1]]^{\mathrm{T}}, \tag{5}$$

with $\mathbf{s}$ the signal vector, $\mathbf{w}$ the noise vector. Then, the 1-bit quantized vector is

$$\mathbf{q} = \mathcal{Q}(\mathbf{y}) = [q[0], q[1], \cdots, q[N-1]]^{\mathrm{T}}. \tag{6}$$

The unquantized $\mathbf{y}$ is gaussian with $\mathbf{y} \sim \mathcal{CN}(\mathbf{0}, \mathbf{R}_{\mathrm{yy}})$, where $\mathbf{R}_{\mathrm{yy}} = \mathbb{E}\{\mathbf{y}\mathbf{y}^{\mathrm{H}}\}$ is the covariance matrix (also the auto-correlation matrix as $\mathbf{y}$ has zero means). Furthermore, let us define a frequency-domain steering vector as

$$\mathbf{v}(f) = \left[1, e^{\frac{\mathbf{j}2\pi}{F_s}f}, e^{\frac{\mathbf{j}4\pi}{F_s}f}, \cdots, e^{\frac{\mathbf{j}2(N-1)\pi}{F_s}f}\right]^{\mathrm{T}}, \tag{7}$$

then the unquantized signal vector $\mathbf{s}$ can be rewritten as

$$\mathbf{s} = \sum\nolimits_{m=1}^{M} \beta_m \mathbf{v}(f'_m), \tag{8}$$

where we have define $\beta_m = \alpha_m[n] e^{-\mathbf{j}2\pi F_m \tau_m}$ and assume $\alpha_m[n]$ remains the same during the sensing window (i.e., the index n is dropped in the expression).

C. Problem Formulation

The M narrow-band frequencies $\{f_m\}_{m=1}^{M}$ are assumed to lie in exactly M sub-bands, i.e., M out of N slices of the interested wideband spectrum are occupied by M PU signals, as depicted in Fig. 2. The objective of the RF sensor is to provide an N-bit digital word representing the states of the spectrum slices. Each bit representing whether a respective slices is occupied or not. For this, we define $2N$ binary hypotheses $\{\mathcal{H}_{0,n}\}_{n=1}^{N}$ and $\{\mathcal{H}_{1,n}\}_{n=1}^{N}$, in which $\mathcal{H}_{0,n}$ denotes the idle state of the n-th slice and $\mathcal{H}_{1,n}$ represents the active state. A detection algorithm can be adopted to classify the observations into $\mathcal{H}_0$ or $\mathcal{H}_1$ for N slices. For each slice, a test statistics χ_n is formulated based on the 1-bit sampled data, and a test decision is given as follows:

$$\begin{cases} \text{Choose } \mathcal{H}_{0,n}, & \text{if } \chi_n < \theta_n, \\ \text{Choose } \mathcal{H}_{1,n}, & \text{if } \chi_n > \theta_n, \end{cases} \quad \text{for } n \in \{1, 2, \ldots, N\}, \quad (9)$$

where θ_n is a decision threshold. The performance of a detection algorithm is evaluated by the detection probability P_d and the false alarm probability P_f. The detection probability is the probability of detecting a active spectrum slice when it is truly occupied by a signal, while the false alarm probability is the probability that the detector incorrectly decides that the spectrum slice as active when it is actually not.

III. The Effects of 1-bit Quantization

With the signal model described in Section II-B, the variance of $[\mathbf{y}]_i$, which equals to the i-th diagonal entry of $\mathbf{R}_{\text{yy}}$, is given by

$$\rho = [\mathbf{R}_{\text{yy}}]_{ii} = \mathbb{E}\{[\mathbf{y}]_i [\mathbf{y}]_i^*\} = \sum\nolimits_{m=1}^{M} |\beta_m|^2 + \sigma_w^2. \quad (10)$$

The correlation between the $[\mathbf{y}]_i$ and $[\mathbf{y}]_j$ is

$$\begin{aligned} \rho_{ij} &= [\mathbf{R}_{\text{yy}}]_{ij} = \mathbb{E}\{[\mathbf{y}]_i [\mathbf{y}]_j^*\} \\ &= \mathbb{E}\left\{ \left[\sum\nolimits_m \beta_m e^{\frac{\mathbf{j}2\pi(i-1)f'_m}{F_s}} \right] \left[\sum\nolimits_m \beta_m^* e^{-\frac{\mathbf{j}2\pi(j-1)f'_m}{F_s}} \right] \right\} \\ &= \sum\nolimits_m |\beta_m|^2 e^{\frac{\mathbf{j}2\pi(i-j)f'_m}{F_s}}. \end{aligned}$$

For the one-bit quantized measurement, according to the signal model, the entities of $\mathbf{q}$ as in (6) has zero mean and unit variance. As a consequence, for its covariance matrix $\mathbf{R}_{\text{qq}} = \mathbb{E}\{\mathbf{q}\mathbf{q}^{\text{H}}\}$, we have $[\mathbf{R}_{\text{qq}}]_{ii} = 1$ for the diagonal elements.

Although the signal is highly distorted after the nonlinear 1-bit sampling, the classical Bussgang theorem [4], [14] reveals that there is a linear relationship between the covariance matrices $\mathbf{R}_{\text{yy}}$ and $\mathbf{R}_{\text{qq}}$. Bussgang theory is a powerful tool for the analysis of Gaussian signals passing through nonlinear devices (e.g., the 1-bit ADC). Specifically, when $\mathbf{y} \sim \mathcal{CN}(\mathbf{0}, \mathbf{R}_{\text{yy}})$ holds, (6) can be linearized as

$$\mathbf{q} = \mathcal{Q}(\mathbf{y}) = \mathbf{B}\mathbf{y} + \mathbf{e}, \quad (11)$$

where $\mathbf{e}$ is the non-Gaussian 1-bit distortion plus noise term, and is uncorrelated with $\mathbf{y}$. The linearization matrix $\mathbf{B}$ is given by $\mathbf{B} = \sqrt{\frac{2}{\pi}} \mathbf{\Sigma}_{\text{y}}^{-\frac{1}{2}}$ with $\mathbf{\Sigma}_{\text{y}} = \text{diag}(\mathbf{R}_{\text{yy}})$ [5]. Furthermore, according to Vleck's arcsine law [15], [16] for 1-bit quantization, we have

$$\mathbf{R}_{\text{qq}} = \frac{2}{\pi} \left[\arcsin\left(\mathbf{\Sigma}_{\text{y}}^{-\frac{1}{2}} \mathbf{R}_{\text{yy}} \mathbf{\Sigma}_{\text{y}}^{-\frac{1}{2}} \right) \right], \quad (12)$$

where $[\arcsin(\mathbf{A})]_{ij} = \arcsin(\Re\{[\mathbf{A}]_{ij}\}) + \mathbf{j}\arcsin(\Im\{[\mathbf{A}]_{ij}\})$, i.e., $\arcsin(\cdot)$ is element-wise. The covariance matrix for the non-Gaussian error term $\mathbf{e}$ is then

$$\mathbf{R}_{\text{ee}} = \frac{2}{\pi} \left[\arcsin\left(\mathbf{\Sigma}_{\text{y}}^{-\frac{1}{2}} \mathbf{R}_{\text{yy}} \mathbf{\Sigma}_{\text{y}}^{-\frac{1}{2}} \right) \right] - \mathbf{B}\mathbf{R}_{\text{yy}}\mathbf{B}^{\text{H}}. \quad (13)$$

According to the signal model presented in II-B, we have $\mathbf{\Sigma}_{\text{y}} = \rho\mathbf{I}$. Let us define the normalized covariance matrix for $\mathbf{y}$ as $\bar{\mathbf{R}}_{\text{yy}} = \frac{1}{\rho}\mathbf{R}_{\text{yy}}$, then one can reconstruct $\bar{\mathbf{R}}_{\text{yy}}$ using

$$\bar{\mathbf{R}}_{\text{yy}} = \sin\left(\frac{\pi}{2} \mathbf{R}_{\text{qq}} \right), \quad (14)$$

where $[\sin(\mathbf{A})]_{ij} = \sin(\Re\{[\mathbf{A}]_{ij}\}) + \mathbf{j}\sin(\Im\{[\mathbf{A}]_{ij}\})$. Noticing that $|[\mathbf{R}_{\text{qq}}]_{ij}| < 1$ for $i \neq j$, $|[\mathbf{R}_{\text{qq}}]_{ij}| = 1$ for $i = j$, and $\sin(\pi x/2)$ can be well approximated by a linear function $\pi x/2$ (as shown in Fig. 3), we can approximate $\bar{\mathbf{R}}_{\text{yy}}$ utilizing

$$\bar{\mathbf{R}}_{\text{yy}} \doteq \frac{\pi}{2}\mathbf{R}_{\text{qq}} + \left(1 - \frac{\pi}{2}\right)\mathbf{I} \triangleq \bar{\mathbf{R}}_{\text{yy}}^{\text{app}}, \quad (15)$$

where the term $\left(1 - \frac{\pi}{2}\right)\mathbf{I}$ is used to correct the approximation error for the diagonal elements. When the RF sensor operator in the low SNR regime, the off-diagonal elements of $\mathbf{R}_{\text{qq}}$ will be much smaller than 1, and the accuracy of (15) is high. In the extreme, when SNR approaches zero, the 1-bit sampled data will be independently and uniformly drawn from the QPSK constellation, and off-diagonal elements of $\mathbf{R}_{\text{qq}}$ become zeros.

The equation (15) implies that for the an eigenvector $\mathbf{v}$ of $\mathbf{R}_{\text{yy}}$ with $\mathbf{R}_{\text{yy}}\mathbf{v} = \lambda\mathbf{v}$, we have

$$\frac{\pi}{2}\mathbf{R}_{\text{qq}}\mathbf{v} \doteq \left(\frac{\lambda}{p} - 1 + \frac{\pi}{2}\right)\mathbf{v}, \quad (16)$$

which implies that the $\mathbf{R}_{\text{qq}}$ and $\mathbf{R}_{\text{yy}}$ have nearly identical eigenvectors, and hence, identical signal and noise spaces, when SNR is low.

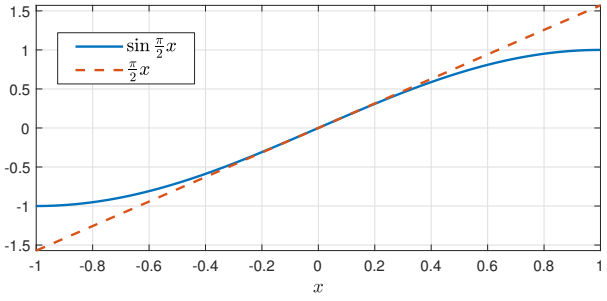

Fig. 3. $\sin(\frac{\pi}{2}x)$ can be well approximated by linear function $\frac{\pi}{2}x$ when x is small, e.g., for $x < \frac{1}{2}$.

IV. Subspace-based 1-bit Wideband Spectrum Sensing Algorithm

To design a wideband spectrum sensing algorithm suitable for low-cost RF sensors, one should consider the computation

complexity, the sensing time, and the detection performance at very low FA probabilities. Here, noticing that the 1-bit covariance matrix $\mathbf{R}_{\rm qq}$ has a similar signal space as with the unquantized one $\mathbf{R}_{\rm yy}$, we present an efficient wideband spectrum sensing algorithm based on subspace techniques. Subspace methods are a class of high-resolution parameter estimation method based on the orthogonality between the signal and noise spaces. Two typical subspace methods are the classical MUltiple SIgnal Classification (MUSIC) [17] method and the estimation of signal parameters via rotational invariance techniques (ESPRIT).

The MUSIC algorithm is widely used for DoA and frequency spectrum estimation. The input of the algorithm is the covariance matrix of the data. We consider the unquantized signal vector $\mathbf{y} = \mathbf{s} + \mathbf{w}$ as in (5), where the noise term $\mathbf{w}$ is assumed to be Gaussian and uncorrelated with the signal part $\mathbf{s}$. Assuming that the number of samples N is larger than the number of frequency components M, the unquantized covariance matrix can be rewritten as

$$\begin{aligned}\mathbf{R}_{\rm yy} &= \mathbb{E}\left\{(\mathbf{s}+\mathbf{w})(\mathbf{s}+\mathbf{w})^{\rm H}\right\} \\ &= \sum\nolimits_{m=1}^{M} \mathbb{E}\left[|\beta_m|^2\right]\mathbf{v}(f'_m)\mathbf{v}^{\rm H}(f'_m) + \mathbb{E}\left\{\mathbf{w}\mathbf{w}^{\rm H}\right\} \\ &= \mathbf{A}\mathbf{\Delta}\mathbf{A}^{\rm H} + \sigma_w^2\mathbf{I} \triangleq \mathbf{S} + \sigma_w^2\mathbf{I},\end{aligned} \tag{17}$$

where $\mathbf{A} = [\mathbf{v}(f'_1), \cdots, \mathbf{v}(f'_M)]$ is a matrix of the frequency steering vectors , and $\mathbf{\Delta} = \mathrm{diag}\left(\mathbb{E}[|\beta_1|^2], \ldots, \mathbb{E}[|\beta_{\rm M}|^2]\right)$. The signal covariance matrix $\mathbf{S} = \mathbf{A}\mathbf{\Delta}\mathbf{A}^{\rm H}$ is a $N \times N$ matrix with a rank M; it therefore has M eigenvectors with nonzero eigenvalues in the signal subspace, and $N-M$ eigenvectors corresponding to the zero eigenvalue. If $\mathbf{u}$ is such an eigenvector in the null space, we have $\mathbf{A}\mathbf{\Delta}\mathbf{A}^{\rm H}\mathbf{u} = \mathbf{0}$, which means $\mathbf{u}^{\rm H}\mathbf{A}\mathbf{\Delta}\mathbf{A}^{\rm H}\mathbf{u} = 0$ and $\mathbf{A}^{\rm H}\mathbf{u} = \mathbf{0}$. This implies that all $N-M$ eigenvectors with zero eigenvalue are orthogonal to all the M steering vectors in $\mathbf{A}$. Let $\mathbf{S} = \mathbf{U}\mathbf{\Lambda}\mathbf{U}^{\rm H}$ be the eigen-decomposition of $\mathbf{S}$. For a eigenvector $\mathbf{v}$ in $\mathbf{U}$, we have $\mathbf{S}\mathbf{v} = \lambda\mathbf{v}$ and $\mathbf{R}_{\rm yy}\mathbf{v} = (\mathbf{S}+\sigma_w^2\mathbf{I})\mathbf{v} = (\lambda+\sigma_w^2)\mathbf{v}$. This implies that $\mathbf{v}$ is also an eigenvector of $\mathbf{R}_{\rm yy}$ with eigenvalue $\lambda + \sigma_w^2$. We thus have the eigen-decomposition $\mathbf{R}_{\rm yy} = \mathbf{U}(\mathbf{\Lambda}+\sigma_w^2\mathbf{I})\mathbf{U}^{\rm H}$ of the unquantized covariance matrix. Based on this eigen-decomposition, we can partition the eigenvector matrix $\mathbf{U}$ into two parts as $\mathbf{U} = [\mathbf{U}_{\rm s}\ \mathbf{U}_{\rm n}]$, where $\mathbf{U}_{\rm s}$ of size $N \times M$ defines the signal subspace, while $\mathbf{U}_{\rm n}$ of size $N \times (N-M)$ defines the noise subspace.

The core idea of MUSIC is to estimate signal parameters using the so-called pseudo-spectrum

$$\mathrm{P}_{\rm pseu}(f) = \frac{1}{\mathbf{v}^{\rm H}(f)\mathbf{U}_{\rm n}\mathbf{U}_{\rm n}^{\rm H}\mathbf{v}(f)} = \frac{1}{\|\mathbf{U}_{\rm n}^{\rm H}\mathbf{v}(f)\|_2^2}. \tag{18}$$

If f equals one of the carrier frequencies of the spectrum components, the denominator is small, and there will be M largest peaks in the pseudo-spectrum. The major limitation of MUSIC is that the number of signal components M should be known as a priori. However, in wideband spectrum sensing, the number of spectrum components M is usually unknown. For this, we utilize the Minimum Description Length (MDL) [18] estimator for determining the number of spectrum components.

Algorithm 1 subspace-based 1-bit wideband spectrum sensing

1: Received 1-bit quantized signal vectors $\{\mathbf{q}_1, \mathbf{q}_2, \ldots, \mathbf{q}_L\}$
2: Estimate the 1-bit quantized covariance matrix by computing $\hat{\mathbf{R}}_{\rm qq} \leftarrow \frac{1}{L}\sum_{l=1}^{L}\mathbf{q}_l\mathbf{q}_l^{\rm H}$
3: Estimate the unquantized normalized covariance matrix via $\hat{\mathbf{R}}_{\rm yy} \leftarrow \frac{\pi}{2}\hat{\mathbf{R}}_{\rm qq} + \left(1-\frac{\pi}{2}\right)\mathbf{I}$
4: Perform the eigen-decomposition $\hat{\mathbf{U}}\hat{\mathbf{\Lambda}}\hat{\mathbf{U}}^{\rm H}$ for $\hat{\mathbf{R}}_{\rm yy}$, where $\hat{\mathbf{U}} = [\mathbf{u}_1, \mathbf{u}_2, \ldots, \mathbf{u}_N]$, and $\hat{\mathbf{\Lambda}} = \mathrm{diag}\{\lambda_1, \lambda_2, \ldots, \lambda_N\}$ with $\lambda_i \geq \lambda_j$ for $i < j$
5: Estimate the number of spectrum components using the MDL estimator, $\hat{M} \leftarrow \arg\min_c \mathrm{MDL}(c, \hat{\mathbf{\Lambda}})$
6: Partition $\hat{\mathbf{U}}$ into $[\mathbf{U}_{\rm s}\ \mathbf{U}_{\rm n}]$ with $\mathbf{U}_{\rm s} = [\mathbf{u}_1, \ldots, \mathbf{u}_{\hat{M}}]$
7: Compute the pseudo-spectrum $\mathrm{P}_{\rm pseu}(f) = \frac{1}{\|\mathbf{U}_{\rm n}^{\rm H}\mathbf{v}(f)\|_2^2}$ for $f \in \{f_1, f_2, \ldots, f_N\}$ which are the center frequencies of the N spectrum slices, and we get a pseudo-spectrum power vector $\mathbf{p}_s = [\mathrm{P}_{\rm pseu}(f_1), \mathrm{P}_{\rm pseu}(f_2), \ldots, \mathrm{P}_{\rm pseu}(f_N)]$
8: Find the $N-\hat{M}$ smallest elements in $\mathbf{p}_s$, estimate the pseudo-spectrum noise floor as $\mathrm{P}_{\rm noise}$, which is the mean of the $N-\hat{M}$ smallest elements in $\mathbf{p}_s$
9: If $p_s(n) > 10^{\frac{\gamma}{10}}\mathrm{P}_{\rm noise}$, mark the n-th slice as occupied

The MDL is an important concept in information theory, it states that one should prefer the model that yields the shortest description of the data when the complexity of the model is considered. Following [18], where MDL is used for estimate the number of signals impinging on a sensor array, the MDL estimator is given by

$$\begin{aligned}\bar{M} &= \arg\min_{c\in\{0,\ldots,N-1\}} \mathrm{MDL}(c, \hat{\mathbf{\Lambda}}) \\ &= \arg\min_{c\in\{0,\ldots,N-1\}} \left\{ -L\log\left(\frac{\prod_{i=c+1}^{N}\lambda_i}{\left(\frac{1}{N-c}\sum_{i=c+1}^{N}\lambda_i\right)^{N-c}}\right) \right. \\ &\qquad \left. +\frac{1}{2}(c(2N-c)+1)\log L \right\},\end{aligned}$$

where $\hat{\mathbf{\Lambda}} = \mathrm{diag}\{\lambda_1, \lambda_2, \ldots, \lambda_N\}$ comprises the eigenvalues of the empirical covariance matrix, with $\lambda_i \geq \lambda_j$ for $i < j$.

To decide whether a spectrum slice is occupied or not, the test statistics χ_n in (9) for the n-th slice is chosen to be $\chi_n = \mathrm{P}_{\rm pseu}(f_n)$ where f_n is the center frequency of the n-th slice. The value of χ_n at a given slice is compared to a threshold. If the value exceeds the threshold, this slice will be marked as occupied. We define a pseudo-spectrum noise floor as the mean of the $N-\hat{M}$ smallest elements in $\mathbf{p}_s = [\mathrm{P}_{\rm pseu}(f_1), \mathrm{P}_{\rm pseu}(f_2), \ldots, \mathrm{P}_{\rm pseu}(f_N)]$, where $\{f_1, f_2, \ldots, f_N\}$ are the center frequencies of the N spectrum slices. The threshold is defined to be γ dB above the pseudo-spectrum noise floor. Algorithm 1 summarizes the proposed 1-bit wideband spectrum sensing procedure. Notice that, in practice, the 1-bit covariance matrix is estimated based on multiple observation snapshots for $\mathbf{q}$, and is given by $\hat{\mathbf{R}}_{\rm qq} = \frac{1}{L}\sum_{i=1}^{L}\mathbf{q}_i\mathbf{q}_i^{\rm H}$, where L stands for the number of snapshots. In total, NL samples are needed for the estimation.

V. Performance Evaluation

We evaluate the proposed 1-bit wideband spectrum sensing method by means of numerical simulations. In the simulation, we consider a CR system with a band of 640 MHz. The sampling rate F_s is set to be 640 MHz, so the 1-bit ADC produces a sample every 1.5625 ns. The whole band is divided into $N = 64$ slices with a bandwidth of 10 MHz, M slices are occupied by M RF narrow-band signals. We assume that one fourth of the slices are occupied, so M = 16 in our simulation setting. The carrier frequency of each signal is assumed to lie at the center of a slice. Each narrow-band signal is passed over flat multi-path fading channel. Narrow-band channel coefficients for the M signals are independent. We average all numerical simulations over 10^3 random channel realizations. We compare the performance of the proposed method with two other typical wideband spectrum sensing method, i.e., FFT-based method and correlation-based method. The SNR here is defined as SNR $\triangleq \sigma_{\rm s}^2/\sigma_{\rm w}^2$. We will investigate the detection probability and false alarm performances under different SNRs, and the effects of the number of snapshots L on those performances. For DFT-based wideband spectrum sensing, the power spectrum is given by

$$\mathrm{P}_{\rm dft}(f_n) = \mathbb{E}\left\{\left|\sum\nolimits_{k=0}^{N-1} q[k]e^{\mathbf{j}2\pi nk/N}\right|^2\right\},$$

where the expectation is taken over different snapshots. For correlation-based wideband spectrum sensing, the power spectrum is given by $\mathrm{P}_{\rm corr}(f_n) = \mathbb{E}\left\{\left|\mathbf{q}^{\rm H}\mathbf{v}(f_n)\right|^2\right\}$.

In Fig. 4, we show examples for the estimated subspace-based pseudo-spectrum power, the DFT-based, and the correlation-based spectrum power, for $f_n \in \{f_1, f_2, \ldots, f_N\}$, with the setting of SNR $=$ 0 dB, and 1-bit sampled data of $L = 32$ snapshots. The performance of a wideband spectrum sensing algorithm highly depends on its capabilities to distinguish the noise floor and the signal power in each sub-band. It is shown in Fig. 4 that the subspace-based pseudo-spectrum has a more distinguishable floor compared to the other two. Given the estimated power spectrum, the P_d and P_f performances depends highly on the chosen threshold. When the threshold decreases, more occupied slices will be detected (P_d would increase), while more unoccupied slices would also be classified as occupied (P_f would also increase). As a result, there is a tradeoff between detection probability and false alarm when choosing the threshold. In following evaluations, we select the threshold to be $\gamma = 3$ dB above the estimated noise floor.

A. Time Resolution versus Detection Performances

The time resolution of the RF sensing is $N \times L \times F_s^{-1}$, it drops as the number of snapshots increases as more time is needed to gather more data samples. Fig. 5 shows the simulation results for the detection and false alarm probabilities as a function of the number of snapshots. It is shown that the detection probability increases while the false alarm rate decreases as more snapshots of data are captures, for various

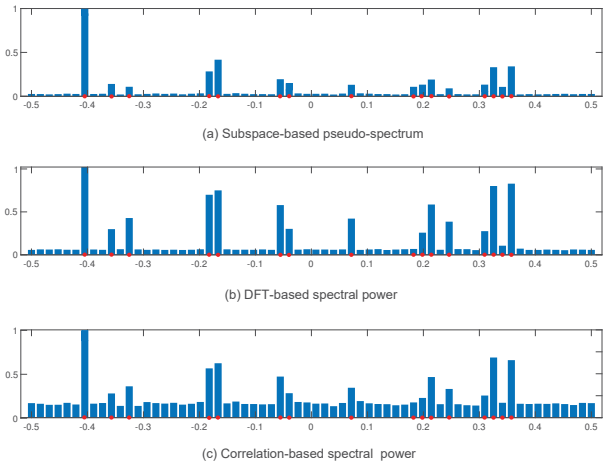

Fig. 4. An example of spectrum power estimation based on 1-bit sampled data, the SNR is set to 0 dB. The number of observation snapshots is L = 32, so there are totally $N \times L = 2048$ 1-bit samples. The values of $\mathrm{P}_{\rm pseu}(f_n)$, $\mathrm{P}_{\rm dft}(f_n)$, $\mathrm{P}_{\rm corr}(f_n)$ have been normalized to lie between 0 and 1.

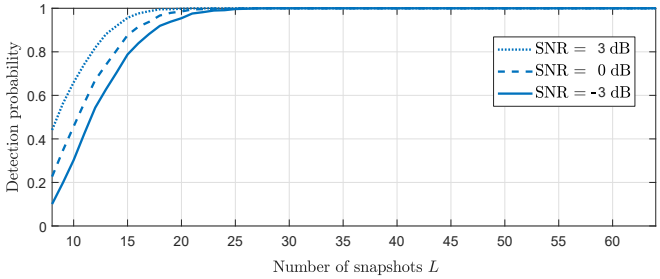

(a) Detection probability versus number of observation snapshots

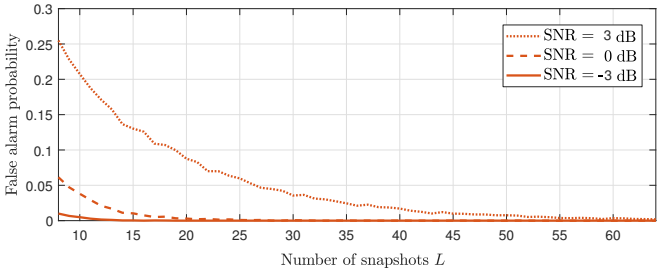

(b) False alarm probability versus number of observation snapshots

Fig. 5. Effects of the number of observation snapshots on the performances of the proposed 1-bit wideband spectrum sensing.

SNR conditions. When SNR is 0, the proposed method can achieve perfect sensing performances with $L = 32$ snapshots, which correspond to a time-resolution of 3.2 μs. It is also interesting to see that, when SNR is high, more snapshots of data are needed to attain a zero false alarm rate. The reason is that in high SNR regime, the distortion resulting from 1-bit sampling dominates the signal-to-noise plus distortion radio (SNDR), and more samples are needed to average out the distortion in estimating the empirical covariance matrix. This implies that 1-bit wideband spectrum sensing has a preferred operational SNR range.

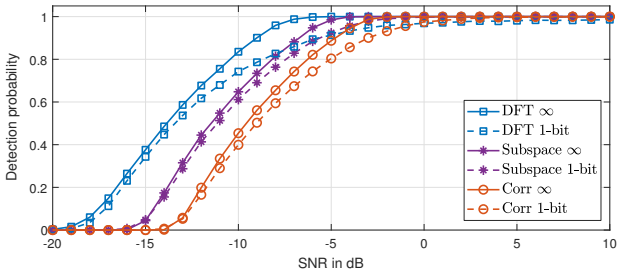

(a) Detection probability performance under different SNR conditions.

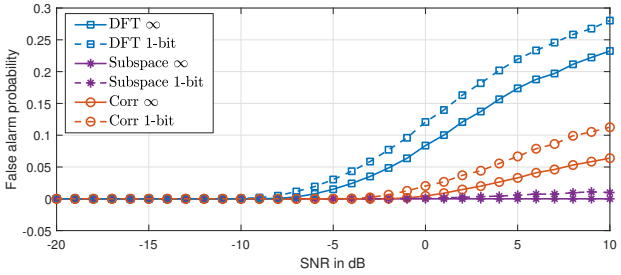

(b) False alarm probability performance under different SNR conditions.

Fig. 6. Effects of SNR on the 1-bit wideband spectrum sensing via the subspace-based, DFT-based and correlation-based methods. Totally $L = 64$ snapshots are adopted. The performances of the corresponding methods with infinite-resolution ADCs are also given for comparison.

B. Performance Comparison under Different SNR *Conditions*

Fig. 6 shows the effects of SNR on the detection performances. As comparisons, the results for DFT-based and correlation-based sensing methods, and the results for all three methods with infinite-resolution ADCs are also given. First, the results indicate that the sensing performances with 1-bit ADCs are comparable to the performances with infinite-resolution ADCs, for all three methods. This is particularly true for the proposed one. In the setting of $L = 64$, the detection probabilities approach 100% when $\mathrm{SNR} > 0$. On the one hand, the detection probability performance of the proposed method is lower than that of DFT-based and higher than correlation-based. On the other hand, the proposed method achieves almost zero false alarm, and is superior compared to the other two. It is worth mentioning that as SNR increases, false alarm rates get higher, especially for DFT-based and correlation-based methods. This is due to the power leakage problem. As signal powers increases, the adjacent vacant spectrum slices would suffer from power leakages from the occupied slices. This problem is severer for the other two methods as compared to the subspace-based method.

VI. Conclusion

We have proposed a subspace-based 1-bit wideband spectrum sensing method, it exhibits ultra-low power consumption, low memory and computation demands, and is suitable for larger-scale RF sensor network deployments. We have analyzed the impact of 1-bit quantization on the wideband spectrum covariance estimation. Our results suggest that the superiority of the subspace technique in parameter estimation translates into efficacy in 1-bit wideband spectrum sensing. We show by simulations that the proposed method exhibits near-zero false alarm while achieves similar detection performances as compared to other typical sensing methods.

Acknowledgments

This work was supported in part by Natural Science Foundation of Jiangsu Province under grant BK20161125, Research Project of National University of Defense Technology under grant ZK-17-03-56.

References

[1] T. Yucek and H. Arslan, "A survey of spectrum sensing algorithms for cognitive radio applications," *IEEE Communications Surveys Tutorials*, vol. 11, no. 1, pp. 116–130, First 2009.

[2] Y. Guddeti, R. Subbaraman, M. Khazraee, A. Schulman, and D. Bharadia, "Sweepsense: Sensing 5 GHz in 5 milliseconds with low-cost radios," in *Proceedings of the 16th USENIX Conference on Networked Systems Design and Implementation*, Feb. 2019, pp. 317–330.

[3] O. B. Akan, O. B. Karli, and O. Ergul, "Cognitive radio sensor networks," *IEEE Network*, vol. 23, no. 4, pp. 34–40, July 2009.

[4] S. Jacobsson, G. Durisi, M. Coldrey, U. Gustavsson, and C. Studer, "Throughput analysis of massive MIMO uplink with low-resolution ADCs," *IEEE Transactions on Wireless Communications*, vol. 16, no. 6, pp. 4038–4051, June 2017.

[5] S. Jacobsson, G. Durisi, M. Coldrey, T. Goldstein, and C. Studer, "Quantized precoding for massive MU-MIMO," *IEEE Transactions on Communications*, vol. 65, no. 11, pp. 4670–4684, Nov 2017.

[6] K. U. Mazher, A. Mezghani, and R. W. Heath, "Low resolution millimeter wave radar: Bounds and performance," in *52nd Asilomar Conference on Signals, Systems, and Computers*, Oct 2018, pp. 554–558.

[7] A. Ameri, J. Li, and M. Soltanalian, "One-bit radar processing and estimation with time-varying sampling thresholds," in *IEEE 10th Sensor Array and Multichannel Signal Processing Workshop (SAM)*, July 2018, pp. 208–212.

[8] C. Liu and P. P. Vaidyanathan, "One-bit sparse array DOA estimation," in *IEEE International Conference on Acoustics, Speech and Signal Processing (ICASSP)*, March 2017, pp. 3126–3130.

[9] O. Bar-Shalom and A. J. Weiss, "DOA estimation using one-bit quantized measurements," *IEEE Transactions on Aerospace and Electronic Systems*, vol. 38, no. 3, pp. 868–884, July 2002.

[10] A. Host-Madsen and P. Handel, "Effects of sampling and quantization on single-tone frequency estimation," *IEEE Transactions on Signal Processing*, vol. 48, no. 3, pp. 650–662, March 2000.

[11] A. Ali and W. Hamouda, "Power-efficient wideband spectrum sensing for cognitive radio systems," *IEEE Transactions on Vehicular Technology*, vol. 67, no. 4, pp. 3269–3283, April 2018.

[12] V. Mishra, S. K. Gupta, Y. K. Verma, V. Ramola, and A. Bora, "A high-gain, low-power latch comparator design for oversampled ADCs," in *5th International Conference on Signal Processing and Integrated Networks (SPIN)*, Feb 2018, pp. 908–913.

[13] A. Giorgetti, M. Chiani, and M. Z. Win, "The effect of narrowband interference on wideband wireless communication systems," *IEEE Transactions on Communications*, vol. 53, no. 12, pp. 2139–2149, Dec 2005.

[14] J. J. Bussgang, "Crosscorrelation functions of amplitude-distorted Gaussian signals," Res. Lab. Elec., Cambridge, MA, USA, Tech. Rep., Mar. 1952.

[15] J. H. Van Vleck and D. Middleton, "The spectrum of clipped noise," *Proceedings of the IEEE*, vol. 54, no. 1, pp. 2–19, Jan 1966.

[16] G. Jacovitti and A. Neri, "Estimation of the autocorrelation function of complex gaussian stationary processes by amplitude clipped signals," *IEEE Transactions on Information Theory*, vol. 40, no. 1, pp. 239–245, Jan 1994.

[17] R. Schmidt, "Multiple emitter location and signal parameter estimation," *IEEE Transactions on Antennas and Propagation*, vol. 34, no. 3, pp. 276–280, Mar 1986.

[18] E. Fishler, M. Grosmann, and H. Messer, "Detection of signals by information theoretic criteria: general asymptotic performance analysis," *IEEE Transactions on Signal Processing*, vol. 50, no. 5, pp. 1027–1036, May 2002.